

¹ **Negative density dependence promotes persistence of a globally rare yet locally**
² **abundant plant species (*Oenothera coloradensis*)**

³ **Abstract**

⁴ 1. Identifying the mechanisms underlying the persistence of rare species has long
⁵ been a motivating question for ecologists. Classical theory implies that commu-
⁶ nity dynamics should be driven by common species, and that natural selection
⁷ should not allow small populations of rare species to persist. Yet, a majority
⁸ of the species found on Earth are rare. Consequently, several mechanisms have
⁹ been proposed to explain their persistence, including negative density dependence,
¹⁰ demographic compensation, vital rate buffering, asynchronous responses of sub-
¹¹ populations to environmental heterogeneity, and fine-scale source-sink dynamics.
¹² Persistence of seeds in a seed bank, which is often ignored in models of population
¹³ dynamics, can also buffer small populations against collapse.

¹⁴ 2. We used integral projection models (IPMs) to examine the population dynam-
¹⁵ ics of *Oenothera coloradensis*, a rare, monocarpic perennial forb, and determine
¹⁶ whether any of five proposed demographic mechanisms for rare species persistence
¹⁷ contribute to the long-term viability of two populations. We also evaluated how
¹⁸ including a discrete seed bank stage changed population models for this species.

¹⁹ 3. Including a seed bank stage in population models had a significant positive impact
²⁰ on modeled *O. coloradensis* population growth rate. Using IPMs that included a
²¹ discrete seedbank state, we found that negative density-dependence was the only
²² supported mechanism for the persistence of this rare species.

²³ 4. *Synthesis:* IPMs of two populations of the rare species *O. coloradensis* emphasize

24 the importance of including cryptic life stages such as seed banks in demographic
25 models, but fail to provide strong support for most of the proposed mechanisms
26 of rare species persistence. We propose that high micro-site abundance in a
27 spatially heterogeneous environment enables this species to persist, allowing it
28 to sidestep the demographic and genetic challenges of small population size that
29 rare species typically face. These results emphasize that globally rare species can
30 employ many different strategies for persistence, including the somewhat counter-
31 intuitive phenomenon of local abundance. This reinforces the need for customized
32 management and conservation strategies that mirror the diversity of mechanisms
33 that allow rare species persistence.

34 **Introduction**

35 Determining how and why populations of rare species persist has been a goal for ecologists
36 since the discipline's inception (Levins & Culver, 1971; Drury, 1974). Theoretically, low
37 population size is a final step on a trajectory toward extinction (Stanley, 1979) or the first
38 step toward ubiquity (Spear, Walsh, Ricciardi, & Vander Zanden, 2021). Yet, small but
39 stable populations of rare species exist in every ecosystem and taxonomic group (Magurran
40 & Henderson, 2011). In fact, a large proportion of species globally – as many as 35% of
41 plant species, for example— can be considered naturally rare (Enquist et al., 2019). The
42 prevalence of rarity suggests it is an evolutionarily stable strategy rather than a stop along
43 the path toward extinction or invasion, and implies that there must be both fundamental
44 and realized niches that are available for rare species to occupy. A growing body of evidence
45 demonstrates the importance of rare species for biological processes, including their impacts

46 on community stability (Arnoldi, Loreau, & Haegeman, 2019), and functional composition
47 (Burner et al., 2022), which in turn impact ecosystem function (Lyons, Brigham, Traut, &
48 Schwartz, 2005).

49 Effective conservation and management of rare species require an understanding of both
50 the conditions causing rarity initially, and the mechanisms that allow rare species to persist.
51 Causes of rarity can vary from highly-specific habitat requirements (Sgarbi & Melo, 2018), to
52 adverse impacts of anthropogenic environmental change (Vincent, Bornand, Kempel, & Fis-
53 cher, 2020). In order to then persist in a state of rarity, a species must overcome any of mul-
54 tiple potential challenges, primarily the negative effects of demographic, environmental, and
55 genetic stochasticity, defined as random variation in vital rates (e.g., survival, reproduction),
56 abiotic conditions, or genetic allele frequencies (May, 1973). Stochastic deleterious events
57 can cause extirpation or even extinction of rare species, since there may not be enough un-
58 affected individuals or subpopulations to “rescue” the affected population (Nei, Maruyama,
59 & Chakraborty, 1975). Rare species that maintain populations over time typically do so
60 by employing demographic strategies that compensate for the adverse effects of small pop-
61 ulation size. There are five main strategies that allow persistence of rare populations (Fig.
62 1) (Dibner, Peterson, Louthan, & Doak, 2019): negative density-dependence (Rovere &
63 Fox, 2019), demographic compensation (Villellas, Doak, García, & Morris, 2015), vital rate
64 buffering (Pfister, 1998; Hilde et al., 2020), asynchronous responses between subpopulations
65 (Abbott, Doak, & Peterson, 2017), and fine-scale source-sink dynamics (Kauffman, Pollock,
66 & Walton, 2004; Pulliam, 1988). Negative density-dependence occurs when the growth
67 rate (λ) of a population increases at small population size. Demographic compensation oc-
68 curs when different vital rates are affected in opposing ways by the same perturbation in

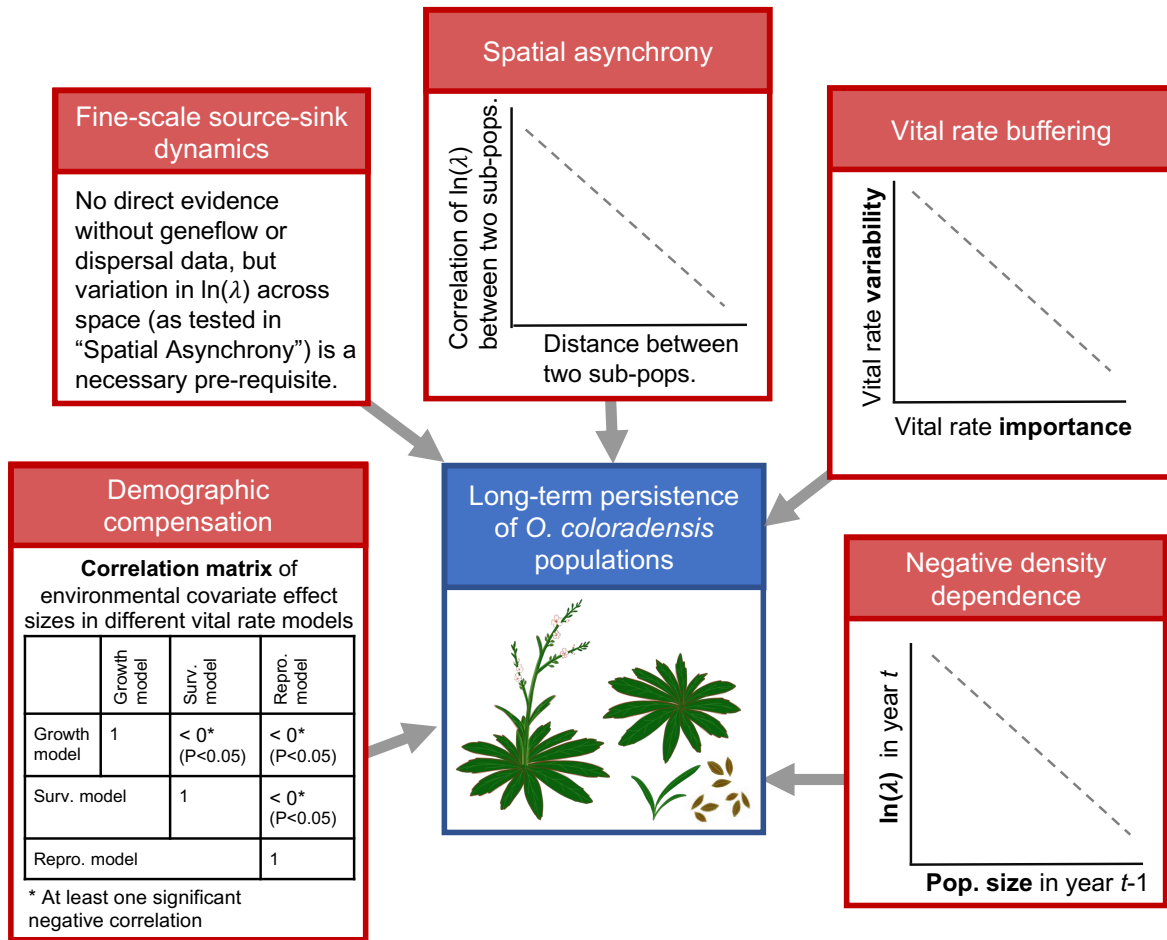
the environment, which can help maintain a relatively constant population λ in response to environmental variation. Vital rate buffering occurs when the variability of vital rates decreases as the vital rate becomes more important(i.e., has a higher elasticity), which prevents negative effects of temporal variation on the λ across time (Tuljapurkar, 1989). Spatial asynchrony occurs when subpopulations close to one another have different or even opposing growth rates, resulting in a stable population-wide λ . Fine-scale source-sink dynamics occur when there is gene flow between subpopulations that bolsters the size and genetic diversity of very small subpopulations, which again results in a stable population-level λ . Each of these mechanisms can act independently, but also can interact or overlap (Dibner et al., 2019).

Here, we identify which of these mechanisms contribute to the persistence or population growth of a rare, endemic plant species, *Oenothera coloradensis* (Rydberg) W.L. Wagner & Hoch (Onagraceae). We use integral projection models (IPMs) (Easterling, Ellner, & Dixon, 2000) that include a discrete seed bank population state. IPMs are flexible models of population dynamics that are constructed using regression models that describe vital rate change across a continuous state variable such as size. IPMs have multiple advantages including better performance with small datasets than traditional matrix models (Ramula, Rees, & Buckley, 2009), and direct incorporation of covariates of interest directly into vital rate models. We built these models with two objectives in mind.

Our first objective was to determine if including information about the seed bank significantly altered population models for *O. coloradensis*. Seed banks can serve as important reservoirs of genetic diversity and buffer populations against collapse (Vitalis, Glémén, & Olivieri, 2004), and can be critical for monocarpic perennials such as *O. coloradensis* that only flower once in their lifetime (Rees et al., 2006). For these reasons, we expected that a

92 soil seed bank is important for *O. coloradensis*, and that its inclusion in IPMs would increase
93 population λ . Seed banks are often not included in population models because their param-
94 eters can be very difficult to estimate, but previous work shows that including them can
95 significantly alter model outcomes (Paniw, Quintana-Ascencio, Ojeda, & Salguero-Gómez,
96 2017; Nguyen, Buckley, Salguero-Gómez, & Wardle, 2019).

97 Our second objective was to identify whether any of the five aforementioned persis-
98 tence mechanisms was acting to maintain *O. coloradensis* populations. This species occurs
99 in habitats that naturally experience frequent, highly localized disturbance, meaning that
100 some subpopulations might be negatively affected by flood, for example, while other nearby
101 subpopulations are simultaneously thriving due to lack of disturbance. Additionally, pre-
102 vious matrix population models constructed for this species in the 1990s found substantial
103 variation in λ across space and time (Floyd & Ranker, 1998). The population-wide pat-
104 tern of asynchronous habitat disturbance also could make source-sink dynamics important.
105 Finally, we have evidence of large fluctuations in the number of plants within subpopula-
106 tions (Heidel, Tuthill, & Wallace, 2021), which suggest that λ decreases at high population
107 size and increases at low population size. Therefore, we predicted that density dependence,
108 small-scale source-sink dynamics and asynchronous responses between subpopulations would
109 be important mechanisms of persistence for *O. coloradensis*.



110 Figure 1: Evidence that would be required to support each of the five mechanisms that can
 111 contribute to long-term viability of small populations of rare species.

112 Materials and Methods

113 Species Description

114 *Oenothera coloradensis* (Onagraceae) (Wagner, Krakos, & Hoch, 2013) is an herbaceous,
 115 monocarpic perennial plant that occurs in frequently disturbed, mesic or wet meadows, and
 116 riparian floodplains (Fertig, 2000). Non-reproductive individuals consist of a rosette of leaves
 117 with a fleshy taproot. Flowering typically occurs after several years, when individuals bolt

and produce a 10-30 cm long floral stalk. Individuals typically die after reproducing—93% of the time in populations we observed. Frequent disturbance such as flooding that reduces competing species and removes litter is important, especially for successful seedling recruitment (Fertig, 2000). All known *O. coloradensis* populations lie within a 7,000-hectare area that includes southeast Wyoming, northern Colorado, and a small part of southwest Nebraska (Fig. S1). The only known population on Federal land occurs on the F. E. Warren Air Force Base near Cheyenne, WY (FEWAFB). The Soapstone Prairie Natural Area (Soapstone), owned by the city of Fort Collins, CO, has the largest known population of *O. coloradensis* individuals (Heidel et al., 2021). The U.S. Fish and Wildlife Service (USFWS) designated *O. coloradensis* as a “threatened” species under the Endangered Species Act in 2000 (Endangered and Threatened Wildlife and Plants, 2000). Managers were concerned that habitat loss due would lead to extinction of this naturally rare species. However, based on subsequent monitoring, the USFWS determined that the species does not appear to be on a trajectory toward extinction, but fluctuates naturally. As a result, *O. coloradensis* was de-listed in 2019. As a result, *O. coloradensis* was de-listed in 2019 (Endangered and Threatened Wildlife and Plants, 2019).

Previous work established that *O. coloradensis* λ is particularly impacted by recruitment of seedlings (Floyd & Ranker, 1998). Seed banks are also likely important, since years of high seedling density are not necessarily preceded by years of high rates of flowering and seed production (Heidel et al., 2021). The *O. coloradensis* seed bank has not been studied directly, but a greenhouse seed study showed that an average of 58% of seeds produced by a parent plant are viable, and that a viable seed has a 20% probability of germinating after two months of cold stratification (Burgess, Hild, & Shaw, 2005). These rates did not change

¹⁴¹ meaningfully over five years (see “Supplementary Material: Species Information” for more
¹⁴² detail).

¹⁴³ **Demographic Data Collection**

¹⁴⁴ We conducted a three-year demographic study of *O. coloradensis* across six spatially dis-
¹⁴⁵ tinct subpopulations, three in the FEWAFB population (“Unnamed creek”, “Crow creek”,
¹⁴⁶ and “Diamond creek”) and three at the Soapstone population (“Meadow”, “HQ3” and
¹⁴⁷ “HQ5”)(Table S1; Fig. S1). In early summer 2018, we established three 2x2 m² quadrats
¹⁴⁸ in each of these subpopulations, resulting in 18 plots (Table S1). Plants larger than 3 cm
¹⁴⁹ are typically “non-seedling” plants at least one year in age. In each study plot, we tagged
¹⁵⁰ and mapped each unique “non-seedling” individual and recorded longest leaf length, re-
¹⁵¹ productive status, and seed production for each (see “Supplementary Information: Seed
¹⁵² Production Estimation” for more detail). Individuals smaller than 3 cm in leaf length are
¹⁵³ typically seedlings that germinated that year, occur at high density, and are less likely to
¹⁵⁴ survive than non-seedling plants. Due to these factors, we tallied seedlings in each plot, but
¹⁵⁵ did not map or tag them. In subsequent 2019 and 2020 censuses, we mapped and tagged new
¹⁵⁶ “non-seedling” individuals, and re-measured all surviving individuals from previous years.
¹⁵⁷ Sample size in a given year at a subpopulation ranged from 48 to 1527 individuals (Table
¹⁵⁸ S1). All mapping, tagging, and leaf measurements took place between late May and early
¹⁵⁹ July, during the peak of vegetative growth for this species.

160 **Environmental Measurements**

161 To determine the effect of temporal variation in climate on *O. coloradensis* populations,
162 we used modeled, population-level temperature and precipitation data from PRISM (PRISM
163 Climate Group; Oregon State University, 2021), which we refer to as "environmental covari-
164 ates". We calculated the mean temperature of both the growing season (April in $year_t$ –
165 August in $year_t$) and preceding winter season (September in $year_{t-1}$ – March in $year_t$) for
166 each year of vital rate data collection at FEWAFB and Soapstone. We also calculated total
167 precipitation for each "water year" (October in $year_{t-1}$ to September in $year_t$), which we used
168 in place of growing season precipitation because the shortgrass steppe ecosystem in which *O.*
169 *coloradensis* occurs receives a majority of its annual precipitation in the form of snow, and
170 melting snow from the previous winter likely drives springtime seedling recruitment. Average
171 temperature of the previous winter is also likely important for seedling recruitment, because
172 seed germination is triggered by cold stratification (Burgess et al., 2005). Growing season
173 temperature and precipitation are likely important for growth, survival, and reproductive
174 output of non-seedling plants.

175 **Vital Rate Models**

176 We used data from the three-year demographic monitoring study detailed above to pa-
177 rameterize models of *O. coloradensis* vital rates (shown in Fig. 2; parameters of fitted vital
178 rate functions are shown in Table S2). We first estimated continuous vital rate functions
179 describing how survival probability, growth, flowering probability, and seed production in
180 $year_{t+1}$ each vary as a function of longest leaf size in $year_t$. We also estimated a continuous

vital rate function describing the distribution of new recruit size in $year_{t+1}$. Finally, we estimated discrete vital rate parameters describing the probability of seeds produced in $year_t$ either entering the seed bank or germinating in $year_{t+1}$, as well as the probability of seeds in the seed bank in $year_t$ either staying in the seed bank or germinating in $year_{t+1}$.

We first created "global" models for each continuous vital rate (Table. 1). We modeled survival probability ($s(z)$) as a function of log-transformed leaf size ($\ln(size_t)$) using generalized linear models with binomial error distributions. Flowering individuals were excluded from the data used to fit survival models, since *O. coloradensis* is a monocarpic perennial that nearly always dies after flowering. We modeled probability of flowering ($Pb(z)$) as a function of using generalized linear models with binomial error distributions, and was predicted by $\ln(size_t)$ plus $\ln(size_t)$ -squared. We modeled seed production ($b(z)$) as a function of $\ln(size_t)$ using negative binomial models because the count data was over-dispersed. We only used data from flowering plants to fit these models, using the "glm.nb" function from the "MASS" R package (Venables & Ripley, 2002). We described growth, or the distribution of plant size in $year_{t+1}$ ($G(z', z)$) as a series of Normal distributions with mean = μ_s and standard deviation = σ_s . μ_s was modeled as a function of $\ln(size_t)$ using a linear model with Gaussian error. σ_s was the residual standard error of this linear model. We described the distribution of recruit size in $year_{t+1}$ ($c_o(z')$) as a Normal distribution with the mean μ_r , and the standard deviation σ_r . μ_r and σ_r were the mean and standard deviation of observed longest leaf size in $year_{t+1}$.

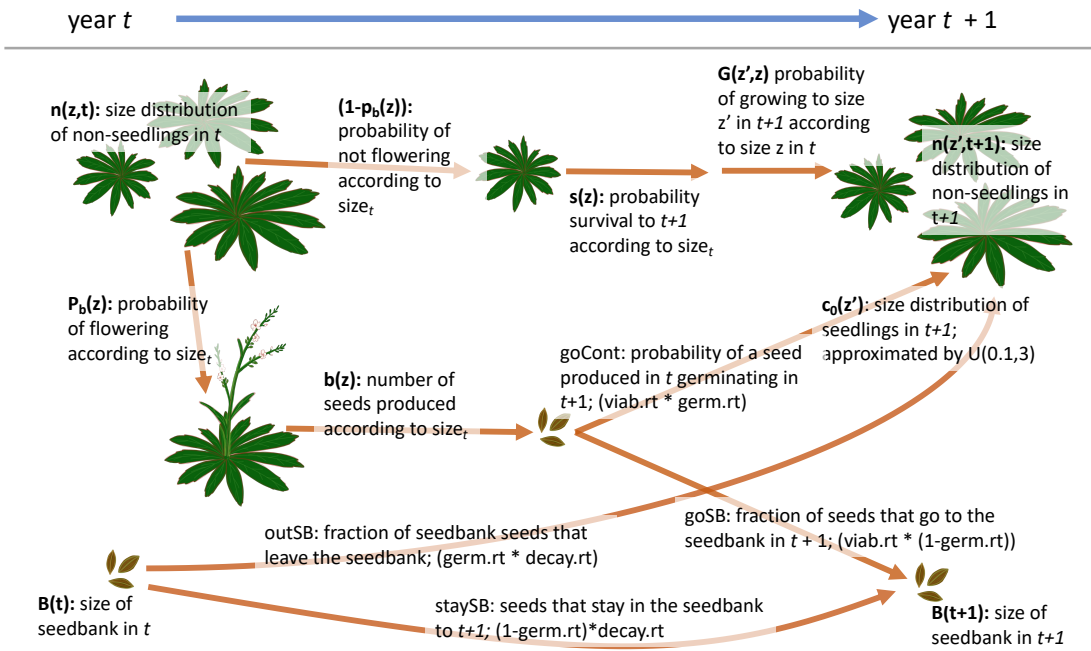
We then used these "global" model structures to fit different versions of continuous vital rate functions, each of which described vital rate processes at different temporal and spatial scales. Models were fit using data from the first transition (2018-2019), the second transition

204 (2019-2020), or pooled across both transitions. We also used data from a single subpopula-
205 tion, a single population, or pooled across both populations. We additionally fit models that
206 expanded on the "global" model structures by including density dependence terms and/or en-
207 vironmental covariates (water year precipitation, mean annual growing season temperature,
208 or mean annual winter temperature). When density dependence or environmental covariates
209 were included, we used AIC model selection to confirm that including these covariates im-
210 proved model fit. All continuous vital rate models, regardless of scale, were parameterized
211 using data from "non-seedling plants" as well as seedlings. We incorporated seedlings into
212 the continuous, non-seedling dataset using a process detailed in "Supplementary Information:
213 Seedling Data."

214 We estimated discrete vital rates for seeds uniformly across both populations and years,
215 using data from both greenhouse and field-based germination and seed viability studies.
216 (Table 1). We did not have the data required to determine how these rates changed across
217 subpopulations or in response to abiotic variation, due to the difficulties of estimating *in situ*
218 seed germination and death. We used the following parameters to estimate discrete seed vital
219 rate parameters: viable seed germination rate (germ. rate) = 0.16, viability rate of seeds
220 produced by a parent plant (viab. rate) = 0.58, rate of natural seed death in the seed bank
221 (death rate) = 0.10 (see "Supplementary Information: Discrete Vital Rate Parameters" for
222 more detail).

227 Population Models

228 We used estimates of discrete and continuous *O. coloradensis* vital rates to parameterize
229 a suite of integral projection models (IPMs) for *O. coloradensis*. We then used these models



223 Figure 2: Diagram of the *O. coloradensis* life-cycle, labeled with notation used in vital rate
 224 equations shown in Table 1. Based on model structures and notation from: (Paniw et al.,
 225 2017; Merow et al., 2014; Ellner et al., 2016). "germ.rt" = germination rate, "viab.rt" =
 226 viability rate, "decay.rt" = decay rate.

230 to address the objectives outlined in the Introduction.

231 *Objective 1: Importance of the Seed bank Stage:* We used two different IPMs to determine
 232 whether explicitly including a discrete seed bank stage in a population model leads to signif-
 233 icantly different outcomes relative to a model without a seed bank stage. We first created a
 234 density-independent IPM using continuous vital rate functions parameterized with data from
 235 both Soapstone and FEWAFFB. This model had a single continuous, size-based population
 236 state, and did not include a seed bank state (Table 2: IPM "A"; Eqn. 1). This IPM used a
 237 kernel structure where the continuous, above-ground population state ($n(z', t + 1)$) at time

Table 1: Description of vital rates used in *O. coloradensis* IPMs

Vital Rate	Description	Model
$pEstab$	$P(\text{seed produced in } year_t \text{ establishes as a seedling in } year_{t+1})$	$pEstab = \frac{\text{Num. new recruits in } year_{t+1}}{\text{Num. seeds produced in } year_t}$
$goCont$	$P(\text{seed produced in } year_t \text{ germinates in } year_{t+1})$	$goCont = \text{viab. rate} \times \text{germ. rate}$
$outSB$	$P(\text{seed bank seed in } year_t \text{ germinates in } year_{t+1})$	$outSB = \text{germ. rate} \times (1 - \text{death rate})$
$goSB$	$P(\text{seed produced in } year_t \text{ goes into the seed bank in } year_{t+1})$	$goSB = \text{viab. rate} \times (1 - \text{germ. rate})$
$staySB$	$P(\text{seed bank seed in } year_t \text{ stays in the seed bank in } year_{t+1})$	$staySB = (1 - \text{germ. rate}) \times (1 - \text{death rate})$
$Survival(s(z))$	$P(\text{survival from } year_t \text{ to } year_{t+1})$	$\text{logit}(\text{survival}) \sim \beta_0 + \beta_1(\ln(\text{size}_t)) + \epsilon$
$Flowering(Pb(z))$	$P(\text{flowering in } year_t)$	$\text{logit}(\text{flowering}) \sim \beta_0 + \beta_1(\ln(\text{size}_t)) + \beta_2(\ln(\text{size}_t)^2) + \epsilon$
$Seed\ prod.(b(z))$	$\text{Seed production in } year_t$	$\exp(\text{seed number}) \sim \beta_0 + \beta_1(\ln(\text{size}_t)) + \epsilon$
$Growth(G(z', z))$	$\text{Distribution of } \ln(\text{longest leaf size}) \text{ in } year_t$	$G(z', z) = N(\mu_s, \sigma_s);$ $\mu_s \sim \beta_0 + \beta_1(\ln(\text{size}_t)) + \epsilon;$ $\sigma_s \sim RSE(\beta_0 + \beta_1(\ln(\text{size}_t)) + \epsilon)$
$Recruit\ size(c_o(z'))$	$\text{Distribution of new recruit size in } year_t$	$c_o(z') = N(\mu_r, \sigma_r);$ $\mu_r = \text{mean}(\text{size of recruits in } t);$ $\sigma_r = \text{stnd. dev. (size of recruits in } t)$

* RSE = residual standard error

²³⁸ $t + 1$ was described by the following equation:

$$n(z', t + 1) = \int_L^U (1 - P_b(z))s(z)G(z', z)n(z, t)dz + pEstab \int_L^U P_b(z)b(z)c_o(z')n(z, t)dz \quad (1)$$

We then created an IPM that included both a continuous, size-based stage for above-ground individuals, and a discrete seed bank state (Table 2: IPM “B”; Eqns. 2 & 3) (Ellner & Rees, 2006; Rees et al., 2006; Paniw et al., 2017). This model used the same continuous vital rate functions as IPM A, but also included discrete values describing the probabilities of seeds produced in $year_t$ germinating or going into the seeds bank in $year_{t+1}$, and the probabilities of seeds in the seed bank in $year_t$ germinating or persisting in the seed bank in $year_{t+1}$. This IPM with two population states used a kernel structure where the continuous, above-ground population state ($n(z', t + 1)$) and the seed bank state ($B(t + 1)$) at time $t + 1$ were described by the following equations:

$$n(z', t + 1) = \int_L^U (1 - P_b(z))s(z)G(z', z)n(z, t)dz + \\ goCont \int_L^U P_b(z)b(z)c_o(z')n(z, t)dz + outSB \quad (2)$$

$$B(t + 1) = goSB \int_L^U P_b(z)b(z)n(z, t)dz + B(t)staySB \quad (3)$$

Table 2: A description of the data used to create each IPM, as well as the covariates included in the vital rate models used in that IPM. $\ln(\lambda)$ estimates and 95% bootstrap confidence intervals of $\ln(\lambda)$ are also shown for each IPM.

IPM	Data Included		Transition	Covariates	$\ln(\lambda)$ (95% CI)
	Each pop.	Each subpop.			

		Continuous state only	Continuous + seed bank state	All subpopulations	Soapstone FEWAFB	Unnamed Creek Diamond Creek Crow Creek Meadow HQ3 HQ5	All Transitions	2018-2019 2019-2020	Density dependence	Environmental covariates	
A	x		x				x			0.27 (0.269, 0.271)	
B		x	x				x			0.65 (0.648, 0.650)	
C	x			x			x			0.48 (0.477, 0.489)	
D	x				x		x			1.13 (1.124, 1.142)	
E	x					x	x			0.74 (0.725, 0.746)	
F	x					x	x			0.54 (0.520, 0.551)	
G	x					x	x			0.395 (0.378, 0.401)	
H	x						x	x		0.53 (0.526, 0.540)	
I	x			x			x		x	0.59 (0.576, 0.637)	
J	x				x		x		x	0.63 (0.611, 0.723)	
K	x				x		x		x	-0.10 (-0.135, 0.063)	
L	x					x	x		x	-0.20 (-0.229, -0.167)	
M	x					x	x		x	1.31 (1.294, 1.354)	
N	x						x	x	x	2.31 (2.297, 2.33)	
S	x			x			x		x	x	0.58
T	x				x		x		x	x	0.51
U	x				x		x		x	x	0.90

V	x			x	x	x	x	-0.27
W	x			x	x	x	x	-0.18
X	x			x	x	x	x	0.76
AA	x	x		x				0.50 (0.497, 0.501)
BB	x		x		x			0.73 (0.729, 0.733)
CC	x			x		x		0.38 (0.370, 0.388)
DD	x			x		x		1.56 (1.545, 1.572)
EE	x			x		x		0.90 (0.864, 0.904)
FF	x			x		x		0.62 (0.592, 0.637)
GG	x			x		x		0.73 (0.727, 0.753)
HH	x			x		x		1.11 (1.108, 1.126)
II	x		x			x		0.50 (0.492, 0.513)
JJ	x			x		x		0.71 (0.692, 0.726)
KK	x			x		x		0.76 (0.739, 0.774)
LL	x			x		x		0.41 (0.378, 0.448)
MM	x			x		x		0.03 (0.013, 0.040)
NN	x			x		x		-0.10 (-0.112, -0.097)

*Note: We did not calculate bootstrap 95% confidence intervals for $\ln(\lambda)$ of models "S" –"X", since only vital rate parameters and not lambda values from these models were used in further analysis.

²⁴⁸ In equations for both types of IPMs, z is the distribution of plant longest leaf size (measured
²⁴⁹ as longest leaf length) in the current year ("size_t"), z' is the distribution of plant longest leaf size
²⁵⁰ in the next year ("size_{t+1}"), and U and L are the upper and lower limits of leaf size. $G(z', z)$
²⁵¹ is the vital rate function describing size_{t+1} as a function of size_t. The vital rate functions $s(z)$,

252 $Pb(z)$, and $b(z)$ describe the relationship between $size_t$ and survival probability of non-flowering
253 plants, flowering probability, and seed production of flowering plants, respectively. $c_o(z')$ is the
254 distribution of aboveground recruit $size_{t+1}$. $goCont$, $outSB$, $goSB$, and $staySB$ are discrete
255 parameters that determine seed bank dynamics. $goCont$ is the probability that a seed produced in
256 year t germinates as a seedling in year $t + 1$, $outSB$ is the probability that a seed from the seed
257 bank in year t germinates as a seedling in year $t + 1$, $goSB$ is the probability that a seed produced
258 in year t goes into the seed bank in year $t + 1$, and $staySB$ is the probability of a seed from the
259 seed bank in year t persisting in the seed bank in year $t + 1$ (Paniw et al., 2017) (Table 1). $pEstab$
260 is the probability that a seed produced in year t establishes as a seedling in year $t + 1$.

261 We used these vital rate functions and discrete parameters to construct discretized IPM kernels,
262 which were numerically implemented using the “midpoint rule” method (Easterling et al., 2000)
263 with 500 bins, an upper size limit corresponding to 120% of the maximum observed longest leaf
264 size and a lower size limit corresponding to 80% of the minimum simulated seedling size of 0.1 cm.
265 We then used eigen analysis of these kernels to estimate the log-transformed asymptotic population
266 growth rate ($\ln(\lambda)$), damping ratio, stable size distribution, and reproductive value (Caswell, 2001;
267 Ellner, Childs, & Rees, 2016). We used 1000 iterations of bootstrap resampling to estimate 95%
268 bootstrap confidence intervals (95% CIs) for each continuous vital rate parameter included in each
269 IPM, as well as each estimate of $\ln(\lambda)$ (Merow et al., 2014; Fieberg, Vitense, & Johnson, 2020).
270 We were unable to estimate CIs for discrete seed bank parameters because they were drawn from
271 a previous publication. We used perturbation analysis to determine the sensitivity and elasticity
272 of $\ln(\lambda)$ to changes in germination rate, viability rate, seed survival rate and each continuous vital
273 rate model (Morris & Doak, 2002). Finally, to determine whether including a discrete seed bank
274 state significantly altered our population model, we compared the asymptotic $\ln(\lambda)$ and associated
275 95% CI between IPM "A" and IPM "B."

276 Objective 2: Evaluating Persistence Mechanisms

277 To evaluate whether any of the demographic mechanisms of rare species persistence outlined in

278 Fig. 1 act in populations of *O. coloradensis*, we fit a series of IPMs that each used different subsets

279 of data as well as additional covariates in vital rate functions to account for density dependence and

280 environmental variation (Table 2: IPMs “C” – “NN”). These IPMs all had a mathematical form

281 equivalent to that of IPM “B” described above, with a discrete seed bank state, and a continuous,

282 size-based stage for above-ground individuals (Eqns. 2 & 3). We then used each of these IPMs, as

283 well as the vital rate functions used to construct them, to evaluate a different persistence mechanism.

284 Details of this process for each persistence mechanism are provided below.

285 *Negative Density Dependence:* In order to determine the importance of density dependence in

286 *O. coloradensis* subpopulations, we used IPMs and vital rate functions that were fit uniquely for

287 each subpopulation using data from both transitions. However, one set of IPMs included population

288 size in the current year in vital rate models, while another set of IPMs did not (density-independent

289 IPMs: “C”–“H” in Table 2; density-dependent IPMs: “I”-“N”). We used AIC to identify significant

290 differences between vital rate models with and without density dependence terms. We also used

291 results from subpopulation-level IPMs (Table 2: IPMs ”CC”-”NN”) for each transition to identify

292 relationships between subpopulation size in $year_t$ and $\ln(\lambda)$ (as in Fig. 1), as well as subpopulation

293 size in $year_t$ and the ratio of population size in $year_{t+1}$ and subpopulation size in $year_t$. In

294 addition to population size information and $\ln(\lambda)$ values from our IPMs, we also used population

295 sizes and $\ln(\lambda)$ values from a previously-published demographic study of *O. coloradensis* at the three

296 FEWAFB subpopulations that we also monitored (Floyd & Ranker, 1998). A negative relationship

297 between population size in $year_t$ and either $\ln(\lambda)$ or the ratio of population size in year $t + 1$ to

298 population size in $year_t$ would provide evidence for negative density dependence. Additionally,

299 significant differences between models with and without population size predictor terms would
300 constitute evidence for density dependence.

301 *Demographic Compensation:* To test for demographic compensation, we calculated the correlation
302 between environmental covariate coefficients in different vital rate models. We used vital rate
303 models that were fit using data from each subpopulation and both transitions, and that included
304 covariates for density dependence and as well as environmental covariates that improved model
305 fit (vital rate models from IPMs “S”-“X” in Table 2). We tested the significance of negative cor-
306 relations between environmental covariate coefficients using a randomization procedure similar to
307 that used by Villegas et al. (2015), where we randomly assigned an environmental covariate coeffi-
308 cient drawn from the observed distribution of values for that coefficient to each vital rate function,
309 calculated a correlation matrix between those coefficients in each vital rate function, and counted
310 the number of negative correlations in that matrix. We repeated this procedure 10,000 times to
311 generate a null distribution of the expected number of negative correlations between environmental
312 coefficients. We compared the observed number of negative correlations to these expected distri-
313 butions to determine statistical significance. We could not test for demographic compensation in
314 discrete seed bank vital rate parameters because we did not know how they varied according to
315 environmental conditions. A negative correlation between coefficients for the same covariate in dif-
316 ferent vital rate models would indicate that demographic compensation was taking place (Villegas
317 et al., 2015; Dibner et al., 2019)(Fig. 1). For example, if soil moisture had a positive effect on
318 growth but a negative effect on survival, this would be evidence for demographic compensation.

319 *Vital Rate Buffering:* We tested for the presence of vital rate buffering in *O. coloradensis* pop-
320 ulations by comparing the variability of vital rates to their importance. We used an approach that
321 scales both the standard deviation (variability metric) and sensitivity (importance metric) of vital
322 rates, allowing for a fair comparison of variability and importance across vital rates with fundamen-

323 tally different relationships between their mean and variance (McDonald et al., 2017). Vital rates
324 that are probabilities are constrained between zero and one and thus typically have small variance
325 as the mean approaches these limits, while other vital rates are only constrained by zero and thus
326 typically have variances that increase as the mean increases (Gaillard & Yoccoz, 2003). To enable
327 a fair comparison between these different categories of vital rates, we calculated their importance
328 and variability metrics in different ways. Importance of probability vital rates corresponded to the
329 logit variance stabilized sensitivity, and variability corresponded to the standard deviation of the
330 logit transformed vital rate values. Importance of non-probability vital rates corresponded to the
331 log-scaled sensitivity (or elasticity), and variability was corresponded to standard deviation of the
332 log-transformed vital rate values (McDonald et al., 2017; Morris & Doak, 2002; Link, William A,
333 Paul F Doherty, Fr., 2002).

334 We used IPM “B” to calculate elasticity or logit VSS values for each discrete and continuous
335 vital rate. We calculated the scaled standard deviation for each continuous vital rate function using
336 the vital rates that were fit uniquely for each subpopulation and each transition (Table 2: IPMs
337 “CC” - “NN”). Because we did not have site-level information about discrete seed bank vital rates,
338 we simulated both the maximum and minimum possible standard deviations for each discrete vital
339 rate. We then proceeded with two comparisons of vital rate variability and importance, one using
340 the maximum possible discrete vital rate standard deviation, and another using the minimum. In
341 order to determine the correlation between a single importance/variability value pair for discrete
342 vital rates and a string of value pairs for continuous vital rate functions, we calculated mean
343 importance and variability values for each continuous vital rate function. A significant negative
344 correlation between the mean or absolute scaled importance (logit VSS or elasticity) and mean or
345 absolute variability (standard deviation of logit or log-transformed vital rates) across all vital rates
346 would constitute support for the presence of vital rate buffering in this species (Fig. 1).

347 *Asynchronous Responses and Source-Sink Dynamics:* To determine whether *O. coloradensis*

348 subpopulations showed asynchronous responses to environmental variation, we made a correlation

349 matrix to determine how change in $\ln(\lambda)$ from year to year was correlated across each subpopulation,

350 using values of $\ln(\lambda)$ derived from IPMs for each subpopulation (Table 2: IPMs “C”-“H”). We used

351 the “mantel()” function from the “vegan” R package to perform a Mantel test, which determined if

352 the Spearman correlation of $\ln(\lambda)$ across subpopulations was significantly related to the Euclidean

353 distance between each subpopulation (Oksanen et al., 2020). A negative relationship between the

354 distance between subpopulations and degree of correlation of $\ln(\lambda)$ would constitute evidence for

355 spatial asynchrony between subpopulations (Fig. 1).

356 Because we did not have information about gene flow between subpopulations of *O. coloradensis*

357 via pollination or seed dispersal, it was impossible to directly measure whether fine-scale source-

358 sink dynamics were acting in these populations. However, because variation in $\ln(\lambda)$ across space

359 is a prerequisite for source-sink dynamics, the tests for spatial asynchrony in subpopulations can

360 also provide evidence for the existence of source-sink dynamics. Again, this would be a negative

361 relationship of distance between subpopulations and correlation of subpopulation $\ln(\lambda)$ (Fig. 1).

362 **Results**

363 **Vital Rate Models**

364 Larger non-reproductive plants were more likely to survive than smaller plants (Fig. 3A).

365 Plants below ~ 7.5 cm were likely to be larger, while plants larger than ~ 7.5 cm were likely to be

366 smaller the following year (Fig. 3 B). Flowering probability was best approximated as a quadratic

367 polynomial, where flowering probability peaked at 12 cm leaf length, and plants with the largest

368 leaves exhibited low flowering probability (Fig. 3 C). The number of seeds that a reproductive

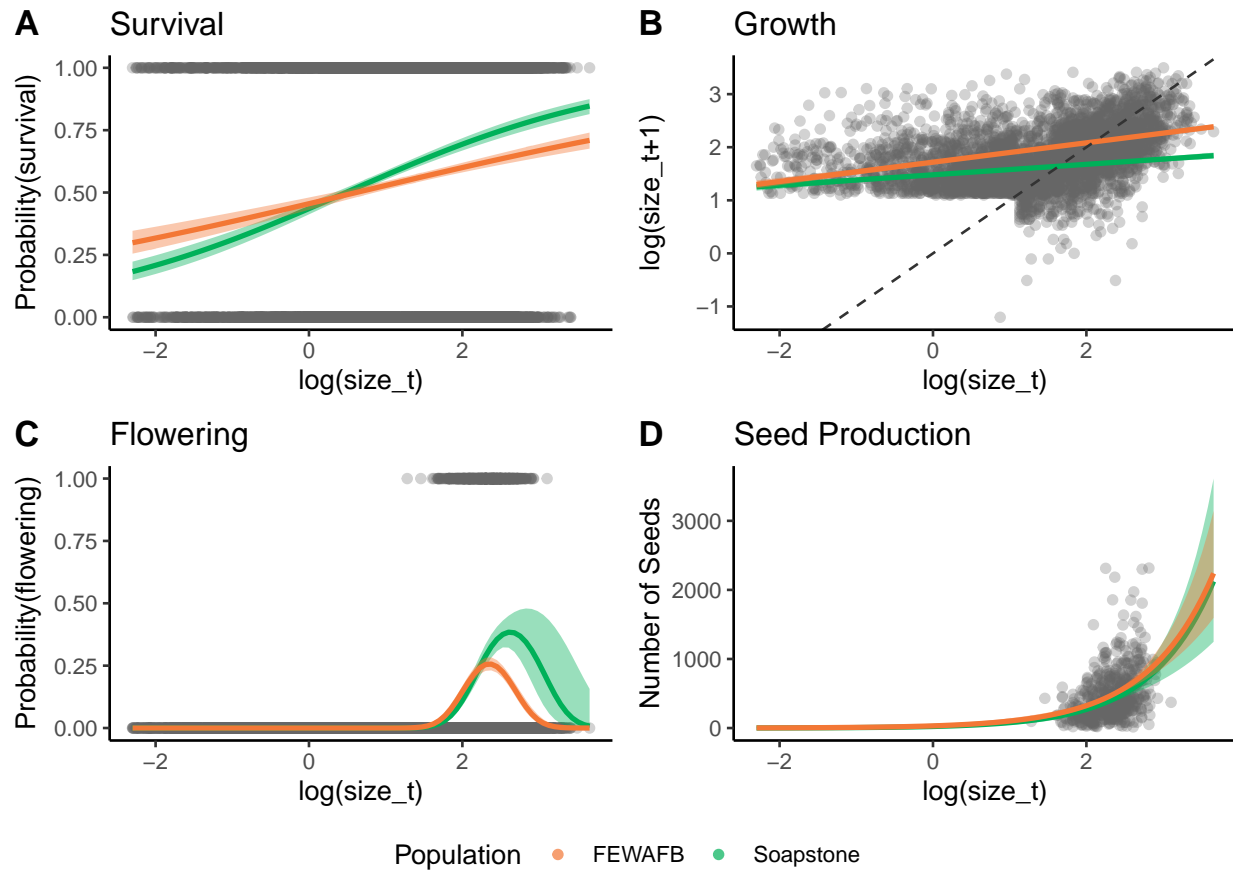
369 plant produced increased sharply with leaf size (Fig. 3 D). The inclusion of additional covariates
370 did not alter the overall shape or sign of the relationships between leaf size and vital rates, so
371 models shown in Figure 3 did not include any additional covariates beyond leaf size.

372 **Objective 1: Importance of the Seed bank Stage**

373 *Integral Projection Models:* We found that including a discrete seed bank stage in IPMs for *O.*
374 *coloradensis* significantly increased $\ln(\lambda)$. The continuous state-only IPM (Table 2: IPM “A”) pre-
375 dicted an asymptotic $\ln(\lambda)$ of 0.27 for all populations (95% CI: 0.269 - 0.271), while the continuous
376 + discrete state IPM (Table 2: IPM “B”) predicted an asymptotic $\ln(\lambda)$ of 0.65 (populations (95%
377 CI: 0.648 - 0.650). All subsequent IPM results refer to models that included a discrete seed bank
378 state.

379 The simplest two-state IPMs that excluded density dependence and environmental variation
380 indicated that both the Soapstone and FEWAFB populations had positive $\ln(\lambda)$ values (Table 2:
381 Soapstone - IPM “AA”, $\ln(\lambda) = 0.50$; FEWAFB – IPM “BB”, $\ln(\lambda) = 0.73$). The Diamond Creek
382 subpopulation at FEWAFB had the highest $\ln(\lambda)$ from 2018 to 2020 (Table 2: IPM “D”, $\ln(\lambda) =$
383 1.13), while the HQ3 subpopulation at Soapstone had the lowest growth rate (Table 2: IPM “G”,
384 $\ln(\lambda) = 0.395$). Almost all additional IPMs identified a positive $\ln(\lambda)$ (Table 2).

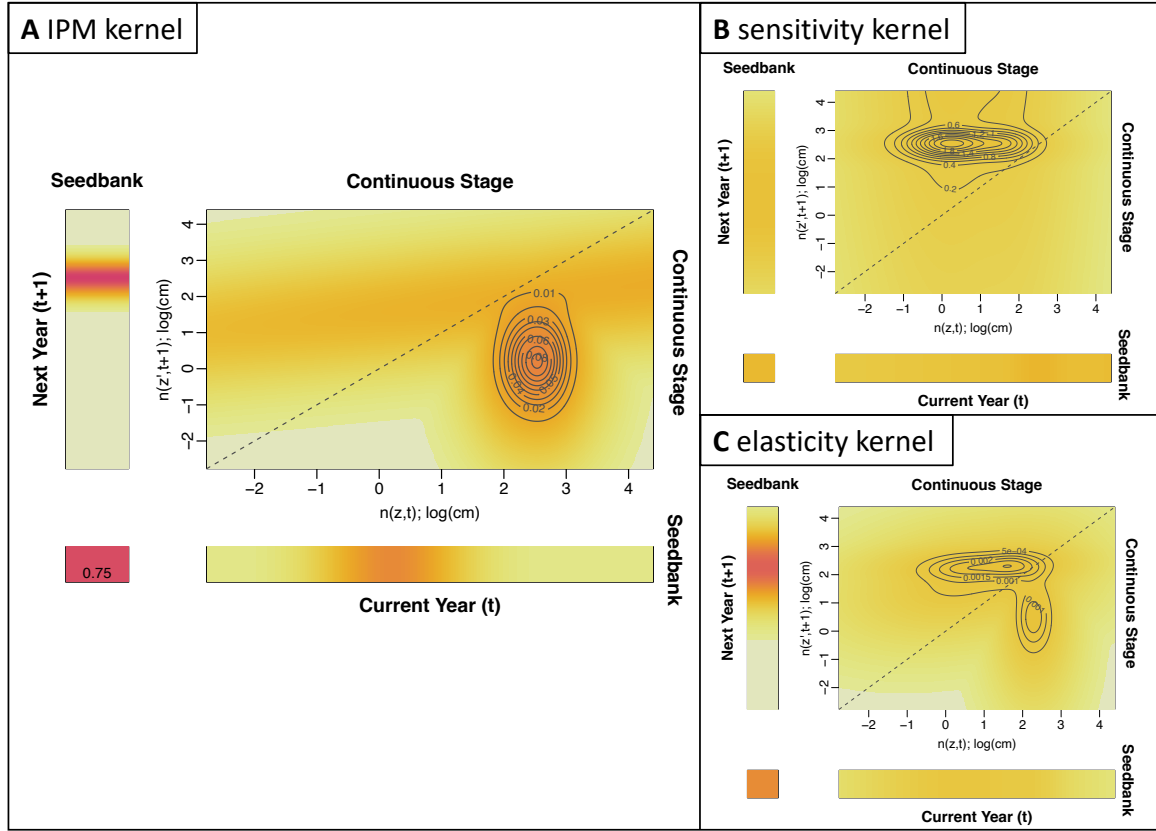
392 A density-independent, discretized IPM kernel (made using IPM “B” in Table 2) calculated
393 transition probabilities within and between the discrete and continuous stages of the *O. coloradensis*
394 life cycle when all populations and transitions were considered together (Fig. 4 A). Relative to other
395 demographic transitions, there was a high probability that seeds stayed in the seed bank, and a
396 high probability that seeds from medium-sized adult plants go into the seed bank in the next year.
397 Population λ was most sensitive to the rates at which seeds were produced by adult plants and
398 stayed in the seed bank (Fig. 4 C).



385 Figure 3: The effect of current year leaf size ($\ln(\text{size}_t)$) on vital rates in monitored *O.*
 386 *coloradensis* populations. Data for all sites and all transitions are shown. Lines indicate
 387 vital rate functions for each population, fit using the "global" model structure described in
 388 the Methods section. Bands around each line show 95% confidence intervals. The dashed
 389 line in panel **B** shows a 1:1 line. The sharp cut-off in $\ln(\text{size}_{t+1})$ in panel **B** is due to the
 390 fact that two-year-old plants could not be seedlings, which were classified as any plant less
 391 than 3 cm in size.

405 Objective 2: Evaluating Persistence Mechanisms

406 *Negative Density Dependence:* We found evidence that negative density-dependence occurred
 407 in subpopulations of *O. coloradensis*. AIC comparison of continuous vital rate models indicated
 408 that density-dependent models were better predictors of the majority of vital rates than density-
 409 independent models in most subpopulations (Table 3). Models that included population size in
 410 the previous year as a covariate were better predictors of growth in five of six subpopulations.



399 Figure 4: Visualizations of the *O. coloradensis* IPM kernels. **(A)** The IPM kernel for *O.*
 400 *coloradensis*. This kernel shows a density-independent IPM constructed using all data from
 401 all transitions (IPM "B"). **(B)** Sensitivity of the IPM kernel. **(C)** Elasticity of the IPM
 402 kernel. In all panels, color indicates probability, with darker colors corresponding to higher
 403 probability, and lighter colors corresponding to lower probability. The dashed line shows a
 404 1:1 line.

411 Density dependent models were better predictors of survival and seed production in four out of
 412 six subpopulations, and density dependent models of flowering were better in one subpopulation.
 413 Recruit size distribution was not affected by density dependence. The vital rate models for the
 414 Meadow population at Soapstone were least affected by density dependence. Although density
 415 dependence was important for *O. coloradensis* in many situations, it appeared only to be acting to
 416 decrease λ at high density (as in the highly dense Diamond Creek or HQ5 subpopulations), but not
 417 clearly increasing lambda at low density (as in the sparsely populated Meadow subpopulation). We

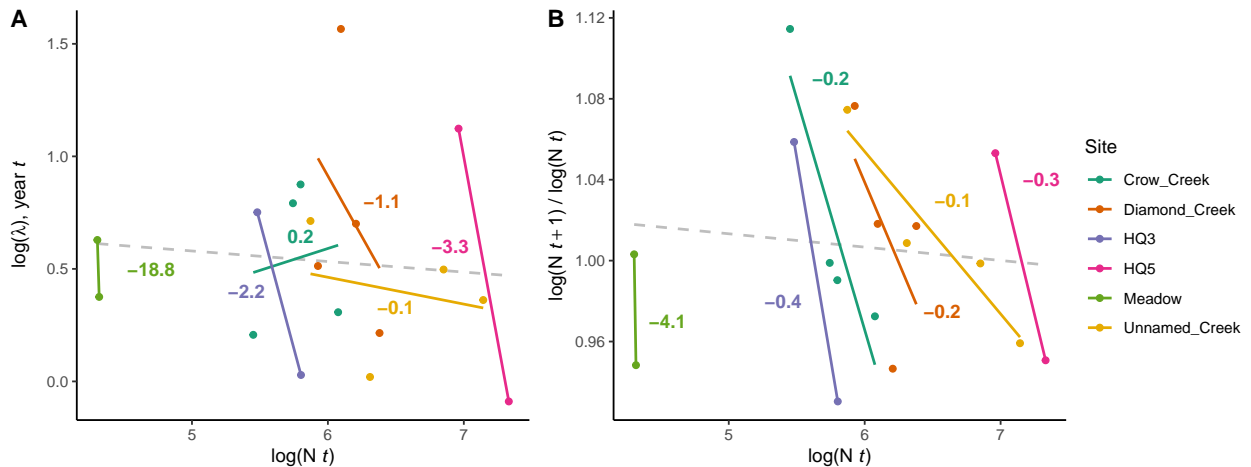
418 also found that, within a subpopulation, $\ln(\lambda)$ was generally higher when subpopulation size was
419 smaller (Fig. 5 A). Similarly, there was a negative relationship within each subpopulation between
420 subpopulation size in $year_t$ and the ratio of subpopulation size in $year_{t+1}$ to subpopulation size in
421 $year_t$ (Fig. 5 B and D); Interestingly, these negative relationships are generally pronounced at the
422 subpopulation level, but are weak when examining data across all subpopulations.

423 *Demographic Compensation:* We did not find evidence of demographic compensation in *O. col-*
424 *oradensis* populations. While there were negative correlations between the effect of mean growing
425 season temperature on vital rates for five combinations of vital rates, none of these correlations
426 were significant (Table 4). The only significant correlation, between temperature coefficients in
427 growth and survival models, was positive. Ten thousand correlations of randomly assigned coef-
428 ficients found that the number of negative correlations in a matrix can be described by a normal
429 distribution with a mean of 4.97 and a standard deviation of 1.60. Using this distribution as a null
430 model, there was a 50.7% probability of observing five negative correlations. Although there is no
431 significant evidence for demographic compensation, it is notable that the effect of mean growing
432 season temperature on distribution of recruit size was negatively correlated with the effect of grow-
433 ing season temperature on all other vital rates. We were only able to compare coefficients across
434 vital rate models for mean growing season temperature, because including precipitation and mean
435 winter temperature as covariates resulted in overfitting in some cases.

452 *Vital Rate Buffering:* We did not find evidence of vital rate buffering in the *O. coloradensis*
453 populations we observed. Vital rate importance (either logistic VSS or elasticity) and variability
454 (corrected SD) were not significantly negatively correlated, regardless of the simulated standard
455 deviation for discrete vital rates we used (Fig. 6; correlation with minimum discrete vital rate SD
456 (**A**): $r = 0.43$, $P = 0.25$; correlation with maximum discrete vital rate SD (**B**): $r = -0.07$, $P =$
457 0.85). As a vital rate became more important for determining $\ln(\lambda)$, it did not become significantly

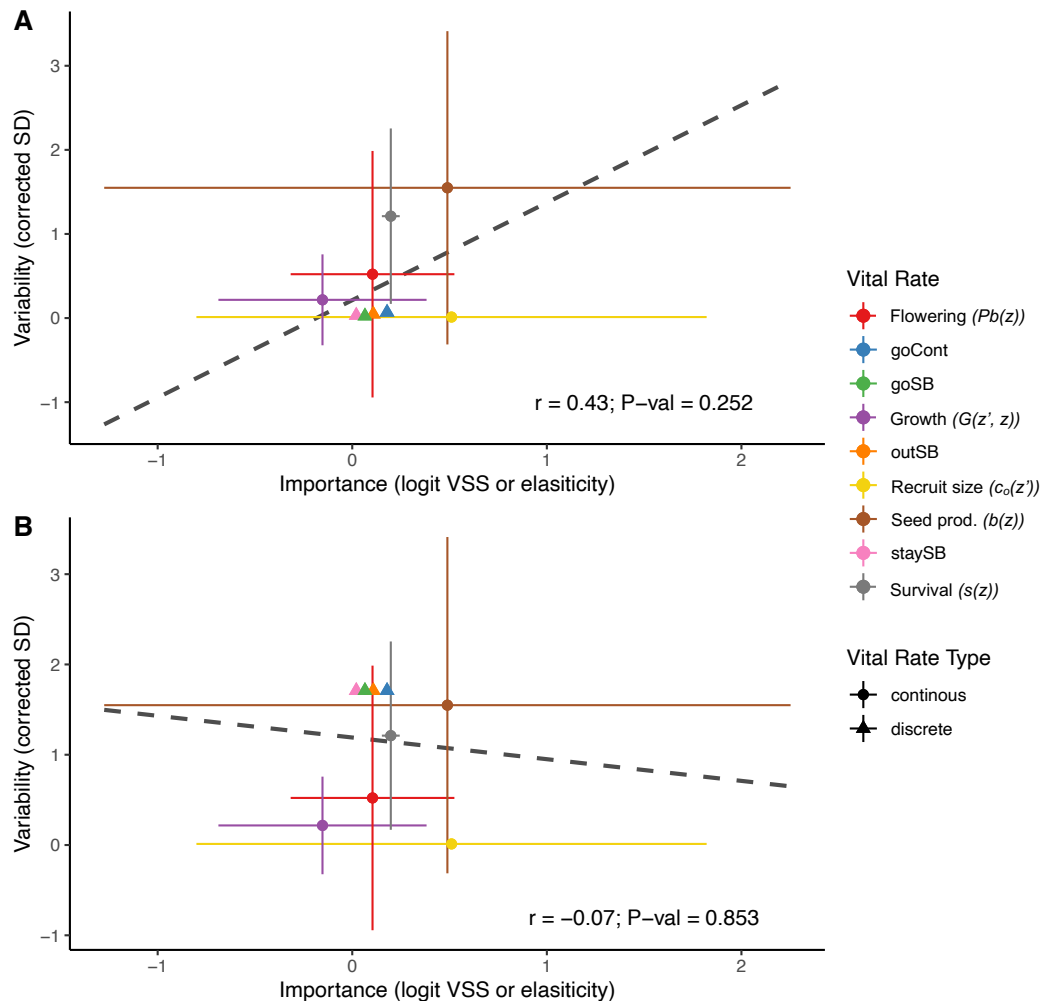
436 Table 3: Comparison of vital rate models with and without density dependence. Values
 437 show the ΔAIC , or difference between the AIC of density independent (DI) and density
 438 dependent (DD) models. Bold text indicates that the $|\Delta\text{AIC}|$ value is > 3 , which means
 439 that including a term for density dependence substantially changed that vital rate model.
 440 A positive $|\Delta\text{AIC}|$ indicates that including density dependence improved the model, while
 441 a negative value indicates that including density dependence made model fit worse. AIC
 442 values for DI and DD values can be found in Table S3.

Vital Rate Model	Subpopulation Data					
	Crow Creek	Diamond Creek	Unnamed Creek	HQ5	HQ3	Meadow
Survival	18.74	107.28	-0.41	320.33	78.82	-0.70
Growth	3.73	22.15	30.811	458.15	30.45	2.66
Flowering	-1.63	-0.44	0.45	54.52	-1.76	-1.72
Seed production	6.41	14.02	-1.29	3.71	4.12	-1.35
Recruit size	-1.93	1.61	-1.93	-1.97	-1.23	-1.99



443 Figure 5: (A) Within the same subpopulation, $\ln(\lambda)$ calculated from IPMs decreases as
 444 population size increases. (B) Within each subpopulation, $\ln(\lambda)$ calculated by change in
 445 population size from year_t to year_{t+1} also decreases as population size increases. In A and B,
 446 each point represents values calculated from data from one transition in one subpopulation.
 447 Solid lines show linear regressions of the relationships between $\ln(N_t)$ and the respective
 448 response variable in each subpopulation. Numbers adjacent to these solid lines show the
 449 slope of each relationship, and are color-coded by subpopulation. Dashed grey lines show
 450 linear regressions of the relationships between $\ln(N_t)$ and the respective response variable
 451 across all subpopulations.

458 less variable, as it would if vital rate buffering was occurring (Fig. 1).



459 Figure 6: The relationship between variability of each vital rate (measured by corrected
 460 standard deviation) and its importance (measured by logit VSS or elasticity) does not show
 461 support for vital rate buffering. **(A)** With the minimum possible simulated discrete vital rate
 462 variability, there is a positive but insignificant correlation between vital rate variability and
 463 importance ($r = 0.43, P = 0.25$). **(B)** Using the maximum possible simulated discrete vital
 464 rate variability, there is a negative but insignificant correlation between vital rate variability
 465 and importance ($r = -0.07, P = 0.85$). Triangles indicate importance and variability for
 466 discrete vital rate parameters, while circles indicates the means of importance and variability
 467 across an entire continuous vital rate function. Error bars around continuous vital rate means
 468 span the the 5th to 95th percentiles of either importance or variability values calculated for
 469 an entire continuous vital rate function. Dashed lines show the correlation between (mean)
 470 variability and (mean) importance across all vital rates.

471 *Asynchronous Responses and Source-Sink Dynamics:* We did not find evidence of asynchronous

472 responses to environmental variation in *O. coloradensis* populations. There was not a significant
473 relationship between the Spearman correlation of $\ln(\lambda)$ between subpopulations and their spatial
474 proximity (Mantel statistic = 0.396, $P = 0.06$). We also performed Mantel tests using $\ln(\lambda)$ cor-
475 relation and distance matrices calculated uniquely for each population, and did not find evidence
476 for asynchronous responses (Soapstone: Mantel statistic = -0.659, $P = 0.83$; FEWAFB: Mantel
477 statistic = 0.798, $P = 0.33$). We did, however, find a positive relationship between correlation of
478 $\ln(\lambda)$ and distance between subpopulations at Soapstone, and a negative relationship between sub-
479 populations at FEWAFB. Collectively, these results fail to provide support for both asynchronous
480 responses and fine-scale source-sink dynamics in these *O. coloradensis* populations.

481 Table 4: Pearson correlations between mean growing season temperature coefficients in each
482 continuous vital rate function. Below each correlation value is the P value for that correla-
483 tion. Bold text indicates a significant correlation.

		Vital Rate				
		<i>Flowering</i>	<i>Survival</i>	<i>Growth</i>	<i>Seed</i>	<i>Recruit</i>
					<i>Prod.</i>	<i>Size</i>
Vital Rate	<i>Flowering</i>	1.00	0.474	0.136	-0.073	-0.786
		(0)	(0.342)	(0.797)	(0.890)	(0.064)
	<i>Survival</i>	1.00	0.886	0.675	-0.3570	
		(0)	(0.019)	(0.141)	(0.237)	
		<i>Growth</i>	1.00	0.664	-0.270	
			(0)	(0.150)	(0.606)	
	<i>Seed Prod.</i>	1.00	-0.432			
		(0)	(0.393)			
	<i>Recruit Size</i>	1.00				
		(0)				

484 **Discussion**

485 Our demographic analysis of the two largest known populations of the globally rare *Oenothera*
486 *coloradensis* evaluated the importance of seed banks to population dynamics and the demographic
487 mechanisms that allow this rare species to persist. We found that including information about
488 cryptic life stages alters the outcomes of the population model (Paniw et al., 2017; Nguyen et
489 al., 2019), and that *O. coloradensis* populations show signs of negative density-dependence at the
490 subpopulation scale (Fig. 5; Table 3). However, these populations do not show substantial evidence
491 of demographic compensation, vital rate buffering, spatial asynchrony, or fine-scale source-sink
492 dynamics. This may indicate that while these mechanisms may be important for the persistence of
493 many small populations of rare plants, they are not strictly necessary in all cases.

494 Including a discrete seed bank state in an IPM increased the asymptotic population growth
495 rate ($\ln(\lambda)$) compared to an IPM with only a continuous, size-based state, although both growth
496 rates were still positive (Table 2: with seed bank: IPM “B”, $\ln(\lambda) = 0.65$; without seed bank:
497 IPM “A”, $\ln(\lambda) = 0.27$). The importance of including the seed bank in the model was consistent
498 with our expectations, and also aligns with the conventional notion that seed banks can act as
499 buffers against stochastic causes of population decline. The discrete rates for the probability of
500 persisting and transitioning out of the seed bank have high elasticity in the IPMs in which they
501 are included, but not the highest elasticity of any vital rate (Fig. 4 C). The rate at which seeds
502 produced by adult plants in $year_t$ go into the seed bank in $year_{t+1}$ is the vital rate function with
503 highest elasticity. Previous matrix population models of *O. coloradensis* without a seed bank state
504 that were constructed in the 1990s identified the emergence rate of new seedlings as the vital rate
505 most important for determining $\ln(\lambda)$ (Floyd & Ranker, 1998). Our finding that seed bank state
506 transitions are important for this species aligns with this previous result, since rate of seedling

507 emergence is the above-ground plant vital rate that is closest to the seed bank in this plant's life
508 cycle. An important caveat to our comparison of models with and without seed bank stages is
509 the fact that the seed bank vital rate parameters we used were inferred from laboratory tests of
510 germination and viability rates, which may be imperfect representations of *in-situ* rates of viability
511 and germination. The annual rate of seed death (10%) was inferred from an *in-situ* study, but
512 is likely imprecise because of low sample size. Regardless of these potential sources of error, our
513 results reinforce the fact that the seed bank can be an important element of a perennial plant's life
514 cycle, and if possible, should be modeled explicitly based on *in-situ* estimates of the probability of
515 seeds going into, persisting in, and emerging from the seed bank.

516 We found evidence that, of the five proposed demographic mechanisms of small population per-
517 sistence, negative density dependence was the only one acting in these *O. coloradensis* populations.
518 Including population size in the previous year as a covariate in vital rate models typically improved
519 model fit, suggesting that density dependence is an important driver of growth, survival, and repro-
520 duction (Table 3). Within a single subpopulation, $\ln(\lambda)$ and the ratio of population size in $year_{t+1}$
521 to $year_t$ was generally higher when population size in $year_t$ was smaller (Fig. 5), which indicates
522 that negative density dependence prevents subpopulations from crashing when their population
523 size is very small. However, this pattern of higher growth rate at low population sizes did not exist
524 when considering all subpopulations together (Fig. 5). This could indicate that each subpopulation
525 is close to its carrying capacity for *O. coloradensis*. This may indicate that the number of indi-
526 viduals is close to carrying capacity in each subpopulation, and that growth rate increases when
527 the population size in a given subpopulation is small in comparison to its subpopulation-specific
528 carrying capacity. *O. coloradensis* vital rates had correlated responses to variation in the abiotic
529 environment (Table 4), which is the inverse of what is expected if demographic buffering is taking
530 place. It is possible that a signal of demographic buffering would appear if we considered different

531 abiotic variables such as disturbance frequency, or had more data. Vital rate buffering also was not
532 identified, either with the minimum or maximum possible simulated discrete vital rate variability
533 (Fig. 6). Vital rates with higher variability (higher SD) did not have a significantly higher or lower
534 importance for determining $\ln(\lambda)$ in comparison to less variable vital rates. This indicates that
535 vital rate buffering is not stabilizing $\ln(\lambda)$ after abiotic or demographic perturbation. The evidence
536 for spatial asynchrony and fine-scale source-sink dynamics was also not strong. Mantel tests did
537 not identify a significant relationship between the correlation of $\ln(\lambda)$ between subpopulations and
538 their spatial proximity, but did identify non-significant relationships between $\ln(\lambda)$ correlation and
539 proximity. However, this relationship was positive in Soapstone prairie subpopulations and negative
540 in FEWAFF subpopulations, which provides inconsistent support for these mechanisms.

541 It is somewhat surprising that negative density dependence is the only mechanism of small
542 population persistence that has significant support in *O. coloradensis* populations, since multiple
543 mechanisms have been identified in at least one other rare species (Dibner et al., 2019). It is possi-
544 ble that support for one or more of these persistence mechanisms could emerge if more information
545 about abiotic variation across space and time and data from more annual transitions was avail-
546 able for analysis. One potential explanation is that, while this species is a globally rare endemic
547 with isolated subpopulations, it often grows at high local density. This strategy, which Rabinowitz
548 describes as “locally abundant in a specific habitat but restricted geographically,” may allow *O.*
549 *coloradensis* to bypass the problems that small populations typically face, such as genetic and demo-
550 graphic bottlenecks that make them susceptible to stochastic environmental variation (Rabinowitz,
551 1981). It has also been shown that rare species are more likely than common species to benefit
552 from facilitative interspecific interactions (Calatayud et al., 2020). *O. coloradensis* may participate
553 in facilitative interactions with other species that increase its probability of persistence, although
554 determining this will require further, community-level analysis. Our results imply that not all rare

555 species can be treated equally. While demographic strategies that help maintain persistence may
556 be effective for some species, other species may employ different strategies. This further emphasizes
557 the importance of carefully considering the specific population and its community dynamics when
558 managing and conserving rare species.

559 Our analysis of the population dynamics of *Oenothera coloradensis* at two distinct locations
560 shows that this species has a life cycle that is strongly driven by introduction and persistence of
561 seeds into a seed bank. More broadly, we show that this rare endemic species shows signs of negative
562 density dependence. Populations of *O. coloradensis* may additionally be maintained via high local
563 abundances that allow them to escape the challenges of small population size that rare species
564 often face (Rabinowitz, 1981). These findings reinforce the importance of careful evaluation of the
565 unique population dynamics of rare species to inform successful conservation and management.

566 References

- 567 Abbott, R. E., Doak, D. F., & Peterson, M. L. (2017). Portfolio effects, climate change,
568 and the persistence of small populations: analyses on the rare plant *Saussurea weberi*.
569 *Ecology*, 98(4), 1071–1081. <https://doi.org/10.1002/ecy.1738>
- 570 Arnoldi, J. F., Loreau, M., & Haegeman, B. (2019). The inherent multidimensionality of
571 temporal variability: how common and rare species shape stability patterns. *Ecology*
572 *Letters*, 22(10), 1557–1567. <https://doi.org/10.1111/ele.13345>
- 573 Burgess, L. M., Hild, A. L., & Shaw, N. L. (2005). Capsule treatments to enhance seedling
574 emergence of *Gaura neomexicana* ssp. *coloradensis*. *Restoration Ecology*, 13(1), 8–14.
575 <https://doi.org/10.1111/j.1526-100X.2005.00002.x>
- 576 Burner, R. C., Drag, L., Stephan, J. G., Birkemoe, T., Wetherbee, R., Muller, J., Siito-
577 ninen, J., Snäll, T., Skarpaas, O., Potterf, M., Doerfler, I., Gossner, M. M., Schall, P.,
578 Weisser, W. W., & Sverdrup-Thygeson, A. (2022). Functional structure of European
579 forest beetle communities is enhanced by rare species. *Biological Conservation*, 267.
580 <https://doi.org/10.1016/j.biocon.2022.109491>

- 581 Calatayud, J., Andivia, E., Escudero, A., Melián, C. J., Bernardo-Madrid, R., Stoffel, M.,
582 Aponte, C., Medina, N. G., Molina-Venegas, R., Arnan, X., Rosvall, M., Neuman,
583 M., Noriega, J. A., Alves-Martins, F., Draper, I., Luzuriaga, A., Ballesteros-Cánovas,
584 J. A., Morales-Molino, C., Ferrandis, P., ... Madrigal-González, J. (2020). Positive
585 associations among rare species and their persistence in ecological assemblages. *Nature
Ecology and Evolution*, 4(1), 40–45. <https://doi.org/10.1038/s41559-019-1053-5>
- 586
- 587 Caswell, H. (2001). *Matrix Population Models: Construction, Analysis, and Interpretation*
588 (2nd ed.). Sinauer Associates.
- 589 Dibner, R. R., Peterson, M. L., Louthan, A. M., & Doak, D. F. (2019). Multiple mechanisms
590 confer stability to isolated populations of a rare endemic plant. *Ecological Monographs*,
591 89(2), 1–16. <https://doi.org/10.1002/ecm.1360>
- 592 Drury, W. H. (1974). Rare species. *Biological Conservation*, 6(3), 162–169. [https://doi.org/10.1016/0006-3207\(74\)90061-5](https://doi.org/10.1016/0006-3207(74)90061-5)
- 593
- 594 Easterling, M. R., Ellner, S. P., & Dixon, P. M. (2000). Size-Specific Sensitivity: Applying
595 a New Structured Population Model. *Ecology*, 81(3), 694–708. [https://doi.org/10.1890/0012-9658\(2000\)081\[0694:SSSAAN\]2.0.CO;2](https://doi.org/10.1890/0012-9658(2000)081[0694:SSSAAN]2.0.CO;2)
- 596
- 597 Ellner, S. P., Childs, D. Z., & Rees, M. (2016). *Data-driven Modelling of Structured Popula-
598 tions*. Switzerland: Springer International Publishing. [https://doi.org/10.1007/978-3-319-28893-2](https://doi.org/10.1007/978-
599 3-319-28893-2)
- 600 Ellner, S. P., & Rees, M. (2006). Integral projection models for species with complex
601 demography. *American Naturalist*, 167(3), 410–428. <https://doi.org/10.1086/499438>
- 602
- 603 *Endangered and threatened wildlife and plants; removing Oenothera coloradensis (colorado
604 butterfly plant) from the federal list of endangered and threatened plants.* (2019). 50
605 C.F.R. pt. 17. ([https://www.federalregister.gov/documents/2019/11/05/2019-24124/endangered-and-threatened-wildlife-and-plants-removing-oenothera-coloradensis-colorado-butterfly](https://www.federalregister.gov/documents/2019/11/05/2019-
606 24124/endangered-and-threatened-wildlife-and-plants-removing-oenothera-
coloradensis-colorado-butterfly))
- 607
- 608 *Endangered and threatened wildlife and plants: Threatened status for the colorado but-
609 terfly plant (Gaura neomexicana ssp. coloradensis) from southeastern wyoming,
610 northcentral colorado, and extreme western nebraska.* (2000). 50 C.F.R. pt. 17.
(<https://www.federalregister.gov/documents/2000/10/18/00-26544/endangered-and->)

- 611 threatened-wildlife-and-plants-threatened-status-for-the-colorado-butterfly-plant)
- 612 Enquist, B. J., Feng, X., Boyle, B., Maitner, B., Newman, E. A., Jørgensen, P. M.,
613 Roehrdanz, P. R., Thiers, B. M., Burger, J. R., Corlett, R. T., Couvreur, T. L.,
614 Dauby, G., Donoghue, J. C., Foden, W., Lovett, J. C., Marquet, P. A., Merow, C.,
615 Midgley, G., Morueta-Holme, N., ... McGill, B. J. (2019). The commonness of rarity:
616 Global and future distribution of rarity across land plants. *Science Advances*, 5(11),
617 1–14. <https://doi.org/10.1126/sciadv.aaz0414>
- 618 Fertig, W. (2000). *Status review of the Colorado butterfly plant (*Gaura neomexicana* ssp.
619 *coloradensis*)* (Tech. Rep.). Laramie, WY: Prepared for U.S. Fish and Wildlife Ser-
620 vice and F. E. Warren Air Force Base by the Wyoming Natural Diversity Database
621 (University of Wyoming).
- 622 Fieberg, J. R., Vitense, K., & Johnson, D. H. (2020). Resampling-based methods for
623 biologists. *PeerJ*, 2020(3). <https://doi.org/10.7717/peerj.9089>
- 624 Floyd, S. K., & Ranker, T. A. (1998). Analysis of a Transition Matrix Model for *Gaura
625 neomexicana* Ssp. *coloradensis* (Onagraceae) Reveals Spatial and Temporal Demo-
626 graphic Variability. *International Journal of Plant Sciences*, 159(5), 853–863.
- 627 Gaillard, J.-M., & Yoccoz, N. G. (2003). Temporal variation in survival of mammals: A case
628 of environmental canalization? *Ecology*, 84(12), 3294–3306.
- 629 Heidel, B., Tuthill, D., & Wallace, Z. (2021). *33-Year Population Trends of Colorado
630 Butterfly Plant (*Oenothera Coloradensis*; Onagraceae), a Short-Lived Riparian Species
631 on F. E. Warren Air Force Base, Laramie County, Wyoming* (Tech. Rep.). Laramie,
632 WY: Prepared for U.S. Fish and Wildlife Service and F. E. Warren Air Force Base by
633 the Wyoming Natural Diversity Database (University of Wyoming).
- 634 Hilde, C. H., Gamelon, M., Sæther, B. E., Gaillard, J. M., Yoccoz, N. G., & Pélabon, C.
635 (2020). The Demographic Buffering Hypothesis: Evidence and Challenges. *Trends in
636 Ecology and Evolution*, 35(6), 523–538. <https://doi.org/10.1016/j.tree.2020.02.004>
- 637 Kauffman, M. J., Pollock, J. F., & Walton, B. (2004). Spatial structure, dispersal, and
638 management of a recovering raptor population. *American Naturalist*, 164(5), 582–597.
639 <https://doi.org/10.1086/424763>
- 640 Levins, R., & Culver, D. (1971). Regional Coexistence of Species and Competition between

- 641 Rare Species. *Proceedings of the National Academy of Sciences*, 68(6), 1246–1248.
642 <https://doi.org/10.1073/pnas.68.6.1246>
- 643 Link, William A, Paul F Doherty, Fr. (2002). Scaling in sensitivity analysis. *Ecology*, 83(12),
644 3299–3305. <https://doi.org/10.2307/3072080>
- 645 Lyons, K. G., Brigham, C. A., Traut, B. H., & Schwartz, M. W. (2005). Rare species
646 and ecosystem functioning. *Conservation Biology*, 19(4), 1019–1024. <https://doi.org/10.1111/j.1523-1739.2005.00106.x>
- 648 Magurran, A. E., & Henderson, P. A. (2011). Commonness and Rarity. In A. E. Magurran
649 & B. J. McGill (Eds.), *Biological diversity : frontiers in measurement and assessment*
650 (pp. 97–104). Oxford University Press.
- 651 May, R. M. (1973). Stability in Randomly Fluctuating Versus Deterministic Environments.
652 *The American Naturalist*, 107(957), 621–650.
- 653 McDonald, J. L., Franco, M., Townley, S., Ezard, T. H., Jelbert, K., & Hodgson, D. J.
654 (2017). Divergent demographic strategies of plants in variable environments. *Nature
655 Ecology and Evolution*, 1(2). <https://doi.org/10.1038/s41559-016-0029>
- 656 Merow, C., Dahlgren, J. P., Metcalf, C. J. E., Childs, D. Z., Evans, M. E., Jongejans, E.,
657 Record, S., Rees, M., Salguero-Gómez, R., & McMahon, S. M. (2014). Advancing
658 population ecology with integral projection models: A practical guide. *Methods in
659 Ecology and Evolution*, 5(2), 99–110. <https://doi.org/10.1111/2041-210X.12146>
- 660 Morris, W. F., & Doak, D. F. (2002). *Quantitative Conservation Biology: Theory and
661 Practice of Population Viability Analysis*. Sunderland, MA: Sinauer Associates.
- 662 Nei, M., Maruyama, T., & Chakraborty, R. (1975). The Bottleneck Effect and Genetic
663 Variability in Populations. *Evolution*, 29(1), 1–10.
- 664 Nguyen, V., Buckley, Y. M., Salguero-Gómez, R., & Wardle, G. M. (2019). Conse-
665 quences of neglecting cryptic life stages from demographic models. *Ecological Mod-
666 elling*, 408(June). <https://doi.org/10.1016/j.ecolmodel.2019.108723>
- 667 Oksanen, J., Blanchet, F. G., Friendly, M., Kindt, R., Legendre, P., McGlinn, D., Minchin,
668 P. R., O'Hara, R. B., Simpson, G. L., Solymos, P., Stevens, M. H. H., Szoecs, E., &
669 Wagner, H. (2020). *vegan: Community Ecology Package*. R package version 2.5-7.
670 Retrieved from <https://cran.r-project.org/package=vegan>

- 671 Paniw, M., Quintana-Ascencio, P. F., Ojeda, F., & Salguero-Gómez, R. (2017). Accounting
672 for uncertainty in dormant life stages in stochastic demographic models. *Oikos*, 126(6),
673 900–909. <https://doi.org/10.1111/oik.03696>
- 674 Pfister, C. A. (1998). Patterns of variance in stage-structured populations : Evolutionary
675 predictions and ecological implications. *Proceedings of the National Academy of Sciences*, 95, 213–218.
- 677 PRISM Climate Group; Oregon State University. (2021). *PRISM Climate Group, Oregon*
678 *State University*. Retrieved from <https://prism.oregonstate.edu>
- 679 Pulliam, H. R. (1988). Sources, Sinks, and Population Regulation. *The American Naturalist*,
680 132(5), 652–661.
- 681 Rabinowitz, D. (1981). Seven forms of rarity. In H. Synge (Ed.), *The biological aspects of*
682 *rare plant conservation*. John Wiley & Sons, Ltd. <https://doi.org/10.2307/4110060>
- 683 Ramula, S., Rees, M., & Buckley, Y. M. (2009). Integral projection models perform better
684 for small demographic data sets than matrix population models: A case study of
685 two perennial herbs. *Journal of Applied Ecology*, 46(5), 1048–1053. <https://doi.org/10.1111/j.1365-2664.2009.01706.x>
- 687 Rees, M., Childs, D. Z., Metcalf, C. J. E., Rose, K. E., Sheppard, A. W., & Grubb, P. J.
688 (2006). Seed dormancy and delayed flowering in monocarpic plants: selective in-
689 teractions in a stochastic environment. *The American Naturalist*, 168(2), E53-E71.
690 <https://doi.org/10.1086/505762>
- 691 Rovere, J., & Fox, J. W. (2019). Persistently rare species experience stronger negative fre-
692 quency dependence than common species: A statistical attractor that is hard to avoid.
693 *Global Ecology and Biogeography*, 28(4), 508–520. <https://doi.org/10.1111/geb.12871>
- 694 Sgarbi, L. F., & Melo, A. S. (2018). You don't belong here: explaining the excess of rare
695 species in terms of habitat, space and time. *Oikos*, 127(4), 497–506. <https://doi.org/10.1111/oik.04855>
- 697 Spear, M. J., Walsh, J. R., Ricciardi, A., & Vander Zanden, M. J. (2021). The Invasion Ecol-
698 ogy of Sleeper Populations: Prevalence, Persistence, and Abrupt Shifts. *BioScience*,
699 71(4), 357–369. <https://doi.org/10.1093/biosci/biaa168>
- 700 Stanley, S. M. (1979). *Macroevolution: Pattern and Process*. W. H. Freeman.

- 701 Tuljapurkar, S. (1989). An Uncertain Life : Demography in Random Environments . *Theoretical
702 Population Biology*, 35, 227–294. [https://doi.org/10.1016/0040-5809\(89\)90001-4](https://doi.org/10.1016/0040-5809(89)90001-4)
- 703 Venables, W. N., & Ripley, B. D. (2002). *Modern Applied Statistics with S* (Fourth ed.).
704 New York: Springer. Retrieved from <https://www.stats.ox.ac.uk/pub/MASS4/>
- 705 Villegas, J., Doak, D. F., García, M. B., & Morris, W. F. (2015). Demographic compensation
706 among populations: What is it, how does it arise and what are its implications? *Ecology
707 Letters*, 18(11), 1139–1152. <https://doi.org/10.1111/ele.12505>
- 708 Vincent, H., Bornand, C. N., Kempel, A., & Fischer, M. (2020). Rare species perform worse
709 than widespread species under changed climate. *Biological Conservation*, 246, 108586.
710 <https://doi.org/10.1016/j.biocon.2020.108586>
- 711 Vitalis, R., Glémén, S., & Olivier, I. (2004). When genes go to sleep: The population genetic
712 consequences of seed dormancy and monocarpic perenniality. *American Naturalist*,
713 163(2), 295–311. <https://doi.org/10.1086/381041>
- 714 Wagner, W. L., Krakos, K. N., & Hoch, P. C. (2013). Taxonomic changes in oenothera
715 sections gaura and calylophus (onagraceae). *PhytoKeys*(28), 61–72. <https://doi.org/10.3897/phytokeys.28.6143>